A New Method for Choosing the Regularization Parameter in Time-Dependent Inverse Problems and Its Application to Magnetocardiography

Jörg Schreiber, Jens Haueisen, *Member, IEEE*, and Jukka Nenonen

Abstract—The current density estimation on the epicardial surface of the heart based on electrocardiographic and magnetocardiographic measurements is one example of an ill-posed inverse problem. Commonly, zeroth-order Tikhonov regularization is applied to solve such problems. A few methods exist for the determination of the critical regularization parameter. However, none of these methods performed sufficiently in our application. In this paper, we propose a new method for choosing a regularization parameter for a time interval. Our basic assumption for this method is that the optimal solution norm must reflect the temporal properties of the magnetic energy. The performance of our method is tested both on simulated data and patient data.

Index Terms—Biomagnetics, boundary-element methods, cardiography, inverse problems.

I. INTRODUCTION

MAGNETOCARDIOGRAPHY (MCG) provides noninvasive information about the electrical activity of the heart [1]. Estimating and imaging the current density distribution on the epicardial surface of the heart can help diagnose myocardial infarction and other heart diseases. The determination of this current density distribution requires the solution of an ill-posed inverse problem. Zeroth-order Thikonov regularization is a commonly applied technique for stabilizing such solutions and leads to the following minimization term:

$$\Delta^2 = \|\mathbf{B} - L\mathbf{j}\|_2^2 + \lambda\|R\mathbf{j}\|_2^2 \qquad (1)$$

where $\mathbf{B}$ is the measured magnetic field vector, L is the leadfield (kernel) matrix, $\mathbf{j}$ is the current density vector, R is the regularization matrix, and λ is the regularization parameter. The equation states that both the residual norm (first term) and the solution norm (second term) should be minimized, whereby the regularization parameter acts as a weight between these terms. The specification of a reasonable value for λ is often very difficult and a few, mainly empirical methods have been proposed [2]–[5]. The L-curve [2] and the χ^2 [3] criteria are two methods
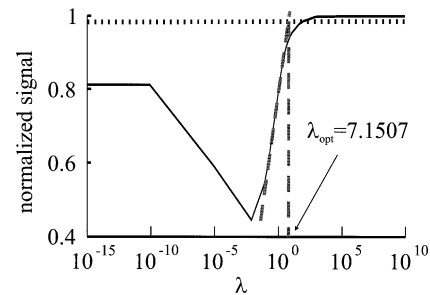
Fig. 1. Normalized MGFP integral (dotted line) and current density solution integral (solid line) over the regularization parameter λ. The gray lines indicate the tangent and the intersection with the MGFP integral in our empirical method for estimating λ.

most frequently used. However, none of these methods performed well in our application consisting of time interval source reconstructions in patients with myocardial infarction.

Analyzing time intervals is of great importance in MCG [and also in magnetoencephalography (MEG)]. A possible approach is to determine the regularization parameter for every time point, but in many cases it is convenient to use a mean value for the entire interval. Based on the assumption that the solution should follow the properties of the magnetic energy of the signal, our aim was to develop an algorithm to determine the regularization parameter.

II. METHODS

A. New Method

The mean global field power (MGFP) is tantamount to the norm of the magnetic field vector, which can be considered as its discrete integral over space. Integrating this value over a certain time leads to a measure of the main magnetic field energy contained in the signal. Analogously, the current density distribution, which depicts the source for this energy, can be considered the same way. From a physical point of view in terms of energy conservation, the normalized MGFP and the current density norm should behave similarly as soon as the optimal regularization parameter λ is met. For example, those parts in the MGFP signal containing zero signals should not contribute to the solution. Thus, we normalized both the MGFP and the current density solution, integrated all values, which were in the time interval considered and above the respective noise levels ($> 3\sigma$), and plotted the two integrals for each λ (Fig. 1). Then, a tangent was fitted to the current density solution integral, such that it represented the maximum curve slope (gray line in Fig. 1).
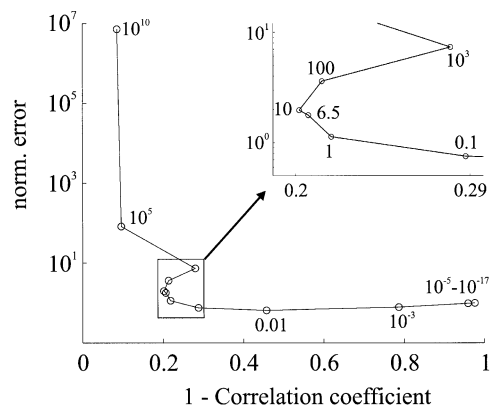
Fig. 2. Normalized squared error over 1—correlation coefficient. The comparison is performed between the strength of the original dipole distribution and the dipole strength of the CDR result.

The optimal parameter λ_{opt} was chosen empirically from the intersection of that tangent with the MGFP integral (dotted line in Fig. 1).

In order to test our method, we performed simulations and analyzed patient data. We compared the results obtained with our method to the results obtained with the often used the L-curve [2] and the χ^2 [3] criteria.

B. Simulations

We modeled the QRS interval (depolarization of the heart, see Fig. 4) of the human heart cycle with the help of 13 dipoles placed around the left ventricle (normal to its surface) representing the basal, medial, and apical slice with each containing the four anatomical directions anterior, lateral, inferior, and septal. The apex was represented by a separate dipole. Each dipole was fixed in direction and the strength varied over time with a Gaussian shape (maximum of 1 μAm), which was shifted for each dipole according to the measurements in [6]. For the field computation, we used a high-resolution boundary-element model including the torso (10-mm triangle side length), the lungs (6 mm) and the ventricles (3 mm) [7]. This model was constructed out of a three–dimensional (3-D) magnetic resonance imaging (MRI) data set of a healthy volunteer. The magnetic field data were calculated in 64 magnetometers arranged in an 8×8 array in front of the torso. The forward calculated fields were disturbed with Gaussian noise using three different noise levels (0.01, 0.05, and 0.1 pT) and provided the input to our minimum norm current density reconstruction (CDR). The optimal regularization parameter, λ_{opt}, was determined by comparing the strength of the solution from the CDR calculations with the strength of the original dipole distribution. We calculated both the correlation coefficient (CC) and the norm square error (NSE) between the values in each source point and for each time point. The optimal parameter results from the plot NSE versus 1-CC (Fig. 2).

C. Patient Data

We tested our new method for determining λ with realistic MCG measurement data [8]. Here, λ_{opt} could be estimated by comparing the CDR with positron emission tomography (PET) data. We used the data of five patients suffering from coronary
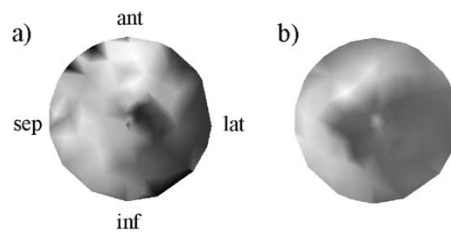

Fig. 3. Bull's eye plots of the left ventricle for (a) positron emission tomography and (b) current density reconstruction data (ant—anterior, sep—septal, lat—lateral, inf—inferior).

artery disease and having a history of myocardial infarction. The presence of coronary artery disease was proven by coronary angiography and wall motion abnormalities in left ventricular angiography. All patients underwent MRI, MCG, and PET imaging within ten days.

MRI data were recorded with a 1.5 T Siemens Magnetom Vision (Siemens, Erlangen, Germany). Thirty-nine ECG-gated contiguous transversal images were recorded during free respiration using a TurboFLASH sequence. The pixel size and the slice thickness were 1.95×1.95 mm and 10 mm, respectively. Patient specific boundary-element models (including triangulated surfaces of the torso, the left and right lungs, the left and right ventricles) were constructed out of the MRI data sets.

PET data were recorded with an ECAT 931/08-12 (Siemens/CTI, Knoxville, TN). A series of 16 contiguous transmission and emission images was recorded. Transmission images were used for the attenuation correction of emission images and also provided topographical information that was utilized for registration purposes. For both transmission and emission images, the pixel size and the slice thickness were 2.41 mm $\times$ 2.41 mm and 6.75 mm, respectively. The PET data were visualized using the common bull's eye plots.

MCG data were recorded by using a 67-channel biomagnetometer with 7 axial and 60 planar first-order gradiometers (Neuromag, Helsinki, Finland). Recordings were taken at rest in supine position. The sampling rate was 1000 Hz. CDRs were performed based on the MCG data and, for the sake of comparison, plotted analogously to the bull's eye plots of the PET data. Fig. 3 shows one example of the PET data and a CDR result. The value for λ_{opt} was determined by the best match between the PET and CDR result. In this procedure, λ was varied manually between 10^{-5} and 10^{+5}.

III. Results

A. Simulations

Although our newly proposed method performed better than the other methods, the χ^2 method produced similar results (Table I). Since only Gaussian noise was used, a good performance of the χ^2 method was expected.

Fig. 4 shows the simulated QRS signal disturbed by 0.1-pT Gaussian noise and the reconstructed current density amplitudes. With increasing λ, the solution norm more closely resembles the MGFP curve, which is not necessarily a sign for a well-chosen regularization parameter. The norm of the original current density distribution (also plotted in Fig. 4) illustrates this fact. Moreover, it becomes clear that even the

TABLE I
SIMULATION RESULTS

Noise level	λ_{opt}	λ_{new}	χ^2 [3]	L-curve [2]
0.01 pT	0.1	0.24	0.59	1.1e-16
0.05 pT	0.5	1.83	4.18	2.08e-17
0.1 pT	0.5	7.15	9.14	2.75e-16

TABLE II
PATIENT DATA RESULTS

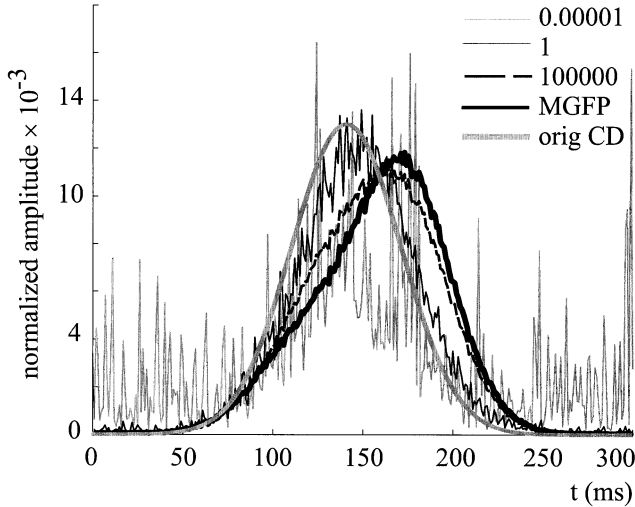| Patient	λ_{opt}	λ_{new}	L-curve [2]
1	0.5	0.13	0.015
2	0.08	0.01	0.006
3	0.03	0.008	0.005
4	0.5	0.2	0.004
5	0.5	0.1	0.01

Fig. 4. Original current density (orig CD), simulated QRS signal (MGFP), and reconstructed current density amplitudes for λ values of 0.000 01, 1, and 100 000. All curves were normalized to their respective integral over the entire time interval.
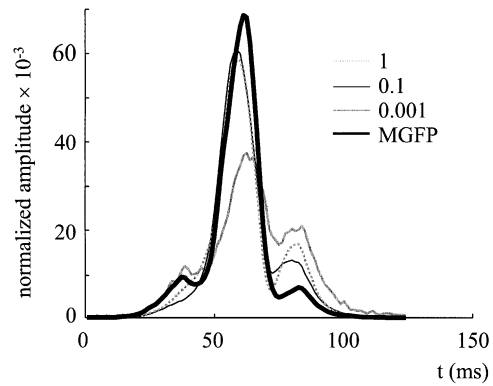

Fig. 5. QRS signal (MGFP) of patient #4 and reconstructed current density amplitudes for λ values of 1, 0.1, and 0.001. All curves were normalized to their respective integral over the entire time interval. The larger amplitudes (y-axis), as compared to Fig. 4, are due to the shorter QRS time interval in this patient.

shape of the MGFP curve and the original source curve can vary considerably inside intervals containing a nonzero signal.

However, since all curves were normalized separately with the help of their respective integrals over time, the absolute amplitudes of the five curves cannot be compared directly. If λ is increased from 1 to 100 000 the squared error will increase dramatically, while the correlation will getting slightly better, like depicted in Fig. 2. This is a consequence of changing the weight of the reconstruction algorithm in favor of minimizing the solution norm. At some points (for a certain regularization parameter) the shape of the reconstructed current density distribution is basically "frozen" and does not exhibit major changes any longer. Only the amplitude is further decreasing when the regularization parameter is increased. As a result the influence of the residual [first term in (1)] vanishes.

B. Patient Data

Again, our new method performed best (Table II), where the L-curve method gave in one case two orders of magnitude, in two cases one order of magnitude, and in two cases less than one order of magnitude of less accurate regularization parameters. The χ^2 method failed since it produced values below 10^{-7} in all cases. Therefore, these values were not included into Table II. The presence of non-Gaussian noise (inherent to real-patient data) most likely yielded the failure of the χ^2 method.

One example of the QRS MGFP signal for patient 4 and the reconstructed current density amplitudes are given in Fig. 5. As in Fig. 4 (simulated data), we observe that the reconstructed current density amplitudes reach their maximum before the QRS signal reaches the maximum. However, the effect is less pronounced in the patient data (Fig. 5).

IV. DISCUSSION

Both simulations and patient data showed that our new method performs better than the commonly applied L-curve and χ^2 methods. However, the optimal regularization parameter was not reached yet in some cases. Therefore, further research will focus on the inclusion of a constraint for temporal smoothness of the solution. Moreover, spatial smoothness in the source space might give additional insight into the correctness of the regularization parameter choice.

For the estimation of λ_{opt} in the five patients, we compared the PET and CDR bull's eye plots only visually. We found the best match between PET and CDR relatively stable for values of λ_{opt} varying around one order of magnitude. We have therefore chosen the respective mean value of λ_{opt} in Table II.

Although our modeling is based on realistic, patient specific geometries employing the boundary-element method, it does not take fiber anisotropy into account. The inclusion of fiber anisotropy can potentially improve current density reconstruction results [9]. Additionally, higher information content of the

MCG data as, e.g., obtained by measurements of all three components of the magnetic vector (currently only one magnetic field component is measured by most commercial devices) will further improve the inverse solution [10], [11].

V. CONCLUSION

We proposed a new method for choosing the regularization parameter in the solution of ill-posed inverse problems with the help of zeroth-order Thikonov regularization. Both simulations and patient data analysis confirmed the superior performance of our method as compared with the commonly applied L-curve method and χ^2 method.

REFERENCES

[1] U. Leder, J. Haueisen, M. Huck, and H. Nowak, "Non-invasive imaging of arrhytmogenic left-ventricular myocardium after infarction," *The Lancet*, vol. 352, p. 1825, 1998.

[2] P. C. Hansen, "Analysis of discrete ill-posed problems by means of the L-curve," *SIAM Rev., Finite Elements Elec. Magn. Field Probl.*, vol. 34, pp. 561–580, 1992.

[3] V. A. Morozov, "The error principle in the solution of operator equations," *USSR Comput. Math. Math. Phys.*, vol. 28, pp. 69–80, 1968.

[4] G. H. Golub, G. Wahba, and M. Heath, "Generalized cross-validation as a method for choosing a good ridge parameter," *Technometrics*, vol. 21, pp. 215–223, 1979.

[5] P. R. Johnston and R. M. Gulrajani, "A new method for regularization parameter determination in the inverse problem of electrocardiography," *IEEE Trans. Bio-Med. Eng.*, vol. 44, pp. 19–39, Jan. 1997.

[6] D. Durrer, R. T. van Dam, G. E. Freud, M. J. Janse, F. L. Meijler, and R. C. Arzbaecher, "Total excitation of isolated human heart," *Circulation*, vol. 41, pp. 899–912, 1970.

[7] J. Haueisen, J. Schreiber, H. Brauer, and T. R. Knösche, "The dependence of the inverse solution accuracy in magnetocardiography on the boundary element discretization," *IEEE Trans. Magn.*, vol. 38, pp. 1045–1048, Mar. 2002.

[8] J. Nenonen, K. Pesola, H. Hänninen, K. Lauerma, P. Takala, and T. Mäkelä *et al.*, "Current-density estimation of exercise-induced ischemia in patients with multivessel coronary artery disease," *J. Electrocardiol.*, vol. 34, pp. 37–42, 2001.

[9] C. Ramon, P. H. Schimpf, Y. Wang, J. Haueisen, and A. Ishimaru, "The effect of volume currents due to myocardial anisotropy on body surface potentials," *Phys. Med. Biol.*, vol. 47, pp. 1167–1184, 2002.

[10] K. Kobayashi and Y. Uchikawa, "Estimation of multiple sources using spatio-temporal data on a three-dimensional measurement of MEG," *IEEE Trans. Magn.*, vol. 37, pp. 2915–2917, July 2001.

[11] C. M. Arturi, L. Di Rienzo, and J. Haueisen, "Information content in single component versus three component cardiomagnetic fields," *IEEE Trans. Magn.*, submitted for publication.